

# THE BELL SYSTEM TECHNICAL JOURNAL

DEVOTED TO THE SCIENTIFIC AND ENGINEERING  
ASPECTS OF ELECTRICAL COMMUNICATION

Volume 50

March 1971

Number 3

Copyright © 1971, American Telephone and Telegraph Company Printed in U.S.A.

## The Energy and General Translation Force of Cylindrical Magnetic Domains

By A. A. THIELE, A. H. BOBECK, E. DELLA TORRE,\* and  
U. F. GIANOLA

(Manuscript received October 7, 1970)

*In this paper we compute the change in the energy of a uniformly magnetized uniaxial platelet produced by the introduction of a cylindrical domain. Differentiation of the energy expression yields the translational force produced by gradients in plate thickness, material composition, or temperature. The force expressions provide a means for estimating the effect of gradients in these parameters on the margins of domain devices. Equating the sum of the gradient produced forces to the drag force yields a general domain velocity expression. The various results are presented in both graphical and tabular form.*

### I. INTRODUCTION

Magnetic memory and logic devices employing cylindrical domains in uniaxial platelets have recently received considerable attention.<sup>1,2</sup> The theory of the static stability of these domains<sup>3</sup> and its application to cylindrical domain devices<sup>4,5</sup> have been discussed in previous papers. This paper is concerned with the translational forces acting on the domains and their effect on device performance.

\* Present address Department of Electrical Engineering, McMaster University, Hamilton, Ontario.

In most device applications, cylindrical domains are propagated by gradients in the applied field.<sup>1,2</sup> Cylindrical domains may, however, be propagated by gradients in any of the independent parameters which determine the total domain energy. These parameters are: the applied field,  $H$ ; the plate thickness,  $h$ ; the saturation magnetization,  $M_s$ ; and the wall energy density,  $\sigma_w$ . The domain radius,  $r_0$ , is not an independent parameter for domains in equilibrium but is determined once the other parameters are specified. The gradients in  $\sigma_w$  and  $M_s$  may be produced by composition gradients, strain gradients or temperature gradients. Composition or thickness gradients may be used to provide forces which are functions of position only, while temperature or strain gradients may be used to provide time variable forces.

The translational force is obtained by differentiation of the total domain energy expression with respect to position, under the assumption that the gradients in the domain parameters which produce the translational force are sufficiently small that the domain remains circular and stable; consequently the energy expression remains valid. Since this method of computing the force is independent of the detailed stress pattern which produces the domain motion, no estimate of the shape distorting tendency of the various parameters is obtained. Equating the sum of the translational forces to the drag force yields the general velocity equation, and comparing the magnitudes of the various forces yields their effects on device operation.

## II. DOMAIN ENERGY

The energy change produced by the introduction of a single isolated circular  $180^\circ$  domain into an infinite plate of uniaxial magnetic material which is otherwise uniformly magnetized along the average plate normal (the  $z$  axis) is now calculated. Such a domain configuration is shown in Fig. 1. The assumptions and notation of Refs. 3, 4 and 5 are maintained except that the domain parameters  $h$ ,  $H$ ,  $M_s$ ,  $\sigma_w$ , and  $r_0$  are allowed to be functions of position on the plate. In particular, the following is assumed in the model: the wall has negligible width, the wall is everywhere parallel to the  $z$  axis, and the wall energy density is independent of wall orientation or curvature. The values of all parameters are assumed to vary sufficiently slowly that they may be represented by their  $z$ -averaged values at the center of the circular domain. Additionally, the applied field is represented by its  $z$  component,  $H$ , since under the assumptions stated above only this component interacts with the magnetization.

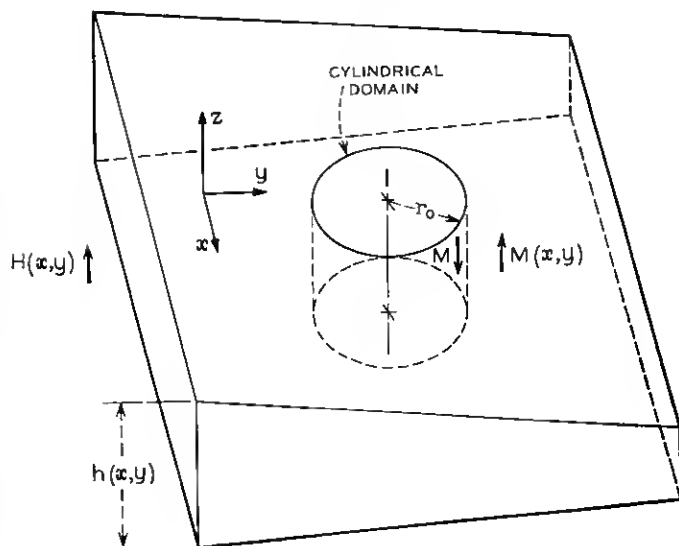


Fig. 1—The cylindrical domain configuration and coordinate system.

The total change in the energy of the system due to the presence of a cylindrical domain is

$$E_T = 2\pi r_0 h \sigma_w + 2M_s H \pi r_0^2 h - 2\pi h^3 (2\pi M_s^2) I(2r_0/h). \quad (1)$$

In this expression the first term, the wall energy, is the product of the wall energy density and the wall area; the second term, the applied field interaction energy, is the product of the magnetization change,  $2M_s$ , the applied field and the domain volume; and the third term, the internal magnetostatic energy, is the negative of the integral of the generalized radial magnetostatic force of Ref. 3. The internal magnetostatic energy function,  $I(2r_0/h)$  is therefore defined as

$$I(2r_0/h) = \int_0^{2r_0/h} F(x) dx, \quad (2)$$

where  $F(x)$  is the force function defined by equations 33 and 138 of Ref. 3. The lower limit of the integral (2) is chosen so that when the plate is uniformly magnetized,  $r_0 = 0$ , the domain energy expression (1) is zero. Various closed form and power series representations of  $I(d/h)$  are given in the appendix of this paper. This function, which is plotted in Fig. 2 as a function of the diameter-to-thickness ratio,  $d/h$ , and is tabulated in Table I, has the asymptotic forms

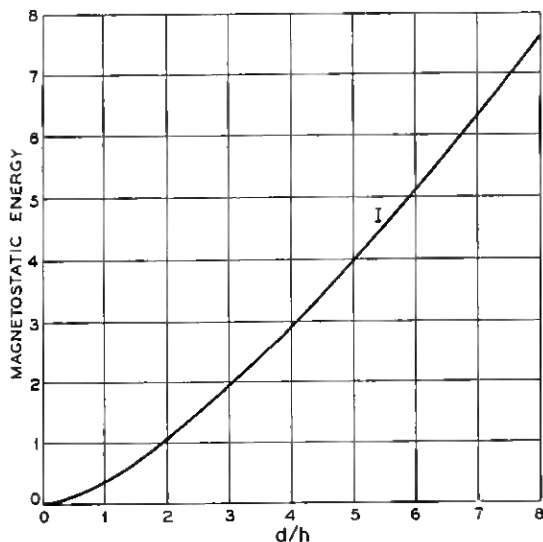


Fig. 2—The internal magnetostatic energy function,  $I$ , as a function of the diameter-to-thickness ratio.

$$I\left(\frac{d}{h}\right) \approx \frac{1}{\pi} \frac{d}{h} \left\{ -\frac{1}{2} + \frac{1}{32} \left(\frac{h}{d}\right)^2 + \left[ 1 + \frac{1}{8} \left(\frac{h}{d}\right)^2 \right] \ln \left| \frac{4d}{h} \right| \right\}, \quad \frac{h}{d} \ll 1 \quad (3a)$$

and

$$I\left(\frac{d}{h}\right) \approx \frac{d}{h} \left[ \frac{1}{2} \left(\frac{d}{h}\right) - \frac{2}{3\pi} \left(\frac{d}{h}\right)^3 + \frac{1}{16} \left(\frac{d}{h}\right)^4 \right], \quad \frac{d}{h} \ll 1. \quad (3b)$$

The physical origin of the asymptotic behavior of the  $I$  function was discussed in some detail in Section IV of Ref. 3.

The domain energy per unit wall length is

$$E_T/\pi d = (2\pi M_s^2)h^2[l/h - J(d/h)], \quad (4)$$

where  $l = \sigma_w/4\pi M_s^2$  is the characteristic material length, where the applied field has been eliminated using the equilibrium condition<sup>3-5</sup>

$$\frac{l}{h} + \frac{d}{h} \frac{H}{4\pi M_s} - F\left(\frac{d}{h}\right) = 0, \quad (5)$$

and where

$$J\left(\frac{d}{h}\right) = 2 \frac{h}{d} I\left(\frac{d}{h}\right) - F\left(\frac{d}{h}\right). \quad (6a)$$

TABLE I—MAGNETOSTATIC ENERGY, FORCE AND STABILITY FUNCTIONS

$d/h$	$I$	$F_H = F$	$S_0$	$S_2$	$F_h = 3J$	$F_M$
0.00	0.	0.	0.	0.	0.	0.
0.10	0.0048	0.0939	0.0059	0.0007	0.0060	0.0979
0.20	0.0184	0.1765	0.0215	0.0028	0.0225	0.1915
0.30	0.0398	0.2493	0.0442	0.0063	0.0474	0.2809
0.40	0.0680	0.3137	0.0716	0.0111	0.0787	0.3662
0.50	0.1023	0.3708	0.1017	0.0172	0.1149	0.4474
0.60	0.1419	0.4216	0.1332	0.0243	0.1544	0.5246
0.70	0.1864	0.4672	0.1648	0.0323	0.1962	0.5980
0.80	0.2352	0.5083	0.1960	0.0411	0.2394	0.6679
0.90	0.2879	0.5455	0.2262	0.0505	0.2832	0.7343
1.00	0.3442	0.5794	0.2552	0.0603	0.3271	0.7975
1.10	0.4037	0.6104	0.2829	0.0705	0.3708	0.8576
1.20	0.4662	0.6390	0.3093	0.0809	0.4139	0.9150
1.30	0.5315	0.6655	0.3343	0.0914	0.4564	0.9698
1.40	0.5993	0.6901	0.3579	0.1020	0.4980	1.0221
1.50	0.6694	0.7130	0.3804	0.1126	0.5386	1.0721
1.60	0.7418	0.7345	0.4016	0.1231	0.5783	1.1200
1.70	0.8163	0.7547	0.4218	0.1336	0.6169	1.1660
1.80	0.8927	0.7737	0.4410	0.1439	0.6546	1.2101
1.90	0.9710	0.7917	0.4592	0.1541	0.6912	1.2525
2.00	1.0510	0.8087	0.4765	0.1642	0.7268	1.2933
2.10	1.1327	0.8249	0.4931	0.1741	0.7615	1.3326
2.20	1.2160	0.8404	0.5089	0.1838	0.7952	1.3705
2.30	1.3008	0.8551	0.5240	0.1933	0.8280	1.4071
2.40	1.3870	0.8692	0.5385	0.2027	0.8599	1.4424
2.50	1.4746	0.8827	0.5524	0.2119	0.8910	1.4766
2.60	1.5635	0.8956	0.5657	0.2209	0.9212	1.5098
2.70	1.6537	0.9081	0.5786	0.2297	0.9507	1.5418
2.80	1.7451	0.9200	0.5909	0.2383	0.9794	1.5729
2.90	1.8377	0.9316	0.6028	0.2468	1.0074	1.6031
3.00	1.9314	0.9427	0.6143	0.2551	1.0347	1.6325
3.20	2.1221	0.9639	0.6362	0.2712	1.0872	1.6887
3.40	2.3169	0.9837	0.6566	0.2866	1.1374	1.7420
3.60	2.5155	1.0024	0.6759	0.3015	1.1853	1.7926
3.80	2.7178	1.0201	0.6940	0.3158	1.2310	1.8407
4.00	2.9235	1.0368	0.7112	0.3295	1.2749	1.8867
4.20	3.1324	1.0526	0.7275	0.3428	1.3170	1.9306
4.40	3.3445	1.0678	0.7430	0.3556	1.3574	1.9727
4.60	3.5595	1.0822	0.7578	0.3679	1.3962	2.0130
4.80	3.7773	1.0960	0.7720	0.3799	1.4337	2.0518
5.00	3.9978	1.1092	0.7855	0.3914	1.4698	2.0891
5.20	4.2209	1.1219	0.7985	0.4026	1.5047	2.1250
5.40	4.4465	1.1341	0.8109	0.4134	1.5383	2.1596
5.60	4.6745	1.1458	0.8229	0.4239	1.5709	2.1931
5.80	4.9048	1.1572	0.8345	0.4341	1.6025	2.2255
6.00	5.1374	1.1681	0.8456	0.4439	1.6331	2.2568
6.20	5.3721	1.1787	0.8564	0.4535	1.6628	2.2872
6.40	5.6088	1.1889	0.8668	0.4629	1.6916	2.3166
6.60	5.8476	1.1988	0.8769	0.4720	1.7196	2.3452
6.80	6.0883	1.2084	0.8866	0.4808	1.7468	2.3730
7.00	6.3310	1.2177	0.8961	0.4894	1.7733	2.3999
7.20	6.5754	1.2268	0.9053	0.4978	1.7991	2.4262
7.40	6.8217	1.2356	0.9142	0.5060	1.8242	2.4518
7.60	7.0696	1.2442	0.9229	0.5140	1.8488	2.4767
7.80	7.3193	1.2525	0.9314	0.5218	1.8727	2.5010
8.00	7.5706	1.2606	0.9396	0.5295	1.8960	2.5247

The function  $J$  has the asymptotic forms

$$J\left(\frac{d}{h}\right) \approx \frac{1}{\pi} \left\{ -\frac{3}{2} - \frac{1}{32} \left(\frac{h}{d}\right)^2 + \left[ 1 + \frac{3}{8} \left(\frac{h}{d}\right)^2 \right] \ln \left| \frac{4d}{h} \right| \right\}, \quad \frac{h}{d} \ll 1 \quad (6b)$$

and

$$J\left(\frac{d}{h}\right) \approx \frac{2}{3\pi} \left(\frac{d}{h}\right)^2 - \frac{1}{8} \left(\frac{d}{h}\right)^3, \quad \frac{d}{h} \ll 1. \quad (6c)$$

The function  $J(d/h)$ , the normalized total magnetostatic energy per unit wall length, is plotted in Fig. 3 together with the force function,  $F(d/h)$  and the stability functions  $S_0(d/h)$  and  $S_2(d/h)$  which have the asymptotic forms

$$F\left(\frac{d}{h}\right) \approx \frac{1}{\pi} \left\{ \frac{1}{2} + \frac{3}{32} \left(\frac{h}{d}\right)^2 + \left[ 1 - \frac{1}{8} \left(\frac{h}{d}\right)^2 \right] \ln \left| \frac{4d}{h} \right| \right\}, \quad \frac{h}{d} \ll 1 \quad (7a)$$

and

$$F\left(\frac{d}{h}\right) \approx \frac{d}{h} - \frac{2}{\pi} \left(\frac{d}{h}\right)^2 + \frac{1}{4} \left(\frac{d}{h}\right)^3, \quad \frac{d}{h} \ll 1, \quad (7b)$$

$$S_0\left(\frac{d}{h}\right) = \frac{1}{\pi} \left\{ -\frac{1}{2} + \frac{13}{32} \left(\frac{h}{d}\right)^2 + \left[ 1 - \frac{3}{8} \left(\frac{h}{d}\right)^2 \right] \ln \left| \frac{4d}{h} \right| \right\}, \quad \frac{h}{d} \ll 1 \quad (8a)$$

and

$$= \frac{2}{\pi} \left(\frac{d}{h}\right)^2 - \frac{1}{2} \left(\frac{d}{h}\right)^3, \quad \frac{d}{h} \ll 1 \quad (8b)$$

and

$$S_2\left(\frac{d}{h}\right) = \frac{1}{\pi} \left\{ -\frac{11}{6} - \frac{17}{96} \left(\frac{h}{d}\right)^2 + \left[ 1 + \frac{5}{8} \left(\frac{h}{d}\right)^2 \right] \ln \left| \frac{4d}{h} \right| \right\}, \quad \frac{h}{d} \ll 1 \quad (9a)$$

and

$$= \frac{2}{9\pi} \left(\frac{d}{h}\right)^2 - \frac{1}{48} \left(\frac{d}{h}\right)^3, \quad \frac{d}{h} \ll 1. \quad (9b)$$

Numerical values of all these functions are given in Table I.

Since from the figure and the asymptotic forms of the functions, (6), (8) and (9),  $J(d/h)$  lies roughly midway (with respect to diameter) between  $S_0(d/h)$  and  $S_2(d/h)$  and since the condition for domain stability is<sup>3-5</sup>  $S_0(d/h) > l/h > S_2(d/h)$ , then a platelet of arbitrary thickness may always be biased such that the introduction of a domain

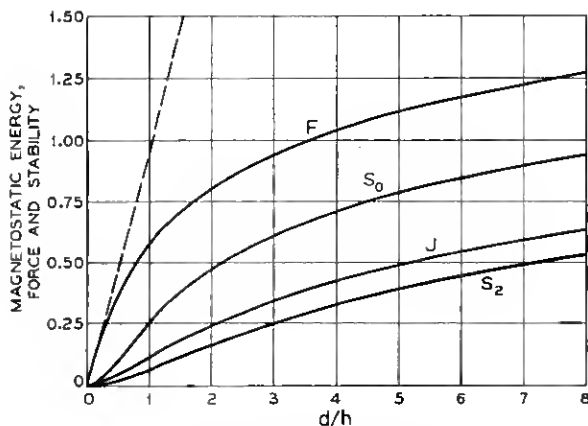


Fig. 3—The magnetostatic energy per unit wall length function,  $J$ , the magnetostatic force function,  $F$ , and the magnetostatic stability functions,  $S_0$  and  $S_2$ , as functions of the diameter-to-thickness ratio.

produces either a positive, or negative, or zero change in the total energy. The force function,  $F(d/h)$ , was included in the figure so that the bias fields yielding these conditions may be determined. The values of the diameters and bias fields of zero energy determined using Fig. 3 or Table I together with (4) and (5) are found to agree with those obtained previously.<sup>6</sup> In the case of a domain having the preferred dimensions,<sup>4,5</sup>  $l/h = 0.2500$  and  $d/h = 2.000$  (corresponding to an applied field of  $H/4\pi M_s = 0.279$ ), then  $J(2.000) = 0.2422$ . Since  $J$  is nearly equal to  $l/h$  the total energy is nearly zero. Under the preferred conditions and in a platelet in which  $4\pi M_s = 100$  Gauss and  $d = 10$  microns, the absolute value of the wall energy and the total magnetostatic energy change are each approximately 0.2 times the rest energy of the electron. [Note that the terms in (4) may not be identified as wall energy and magnetostatic contributions because the equilibrium condition was used to eliminate the applied field.]

### 111. THE TRANSLATIONAL FORCE

The translational force is given by

$$\begin{aligned} \mathbf{F} &= -\nabla E_T, \\ &= -\left(\frac{\partial E_T}{\partial h}\right)_{H, M_s, \sigma_w, r_0} \nabla h - \left(\frac{\partial E_T}{\partial H}\right)_{h, M_s, \sigma_w, r_0} \nabla H \end{aligned}$$

$$\begin{aligned}
& - \left( \frac{\partial E_T}{\partial M_s} \right)_{h, H, \sigma_w, r_0} \nabla M_s - \left( \frac{\partial E_T}{\partial \sigma_w} \right)_{h, H, M_s, r_0} \nabla \sigma_w \\
& - \left( \frac{\partial E_T}{\partial r_0} \right)_{h, H, \sigma_w, M_s} \nabla r_0.
\end{aligned} \quad (10)$$

In this expression  $h$ ,  $H$ ,  $M_s$  and  $\sigma_w$  are considered to be independent variables (functions of position on the platelet) and  $r_0$  is a dependent function of these variables determined by the equilibrium condition (5). Since the fundamental equilibrium condition is  $(\partial E_T / \partial r_0)_{h, H, \sigma_w, M_s} = 0$ , the last term in equation (10) may be dropped. Evaluating the remaining terms using equations (1) and (2) yields

$$\begin{aligned}
\mathbf{F} = & - [2\pi r_0 \sigma_w + 2M_s H \pi r_0^2 - 6\pi h^2 (2\pi M_s^2) I(2r_0/h) \\
& + 4\pi r_0 h (2\pi M_s^2) F(2r_0/h)] \nabla h - [2M_s \pi r_0^2 h] \nabla H \\
& - [2H \pi r_0^2 h - 4\pi h^3 (2\pi M_s) I(2r_0/h)] \nabla M_s \\
& - [2\pi r_0 h] \nabla \sigma_w.
\end{aligned} \quad (11)$$

Eliminating the applied field using the equilibrium condition (5) and rearranging yields

$$\begin{aligned}
\mathbf{F} = & \pi dh^2 (2\pi M_s^2) \{ -[l/h - F_h(d/h)] \nabla h/h + [l/h - F_H(d/h)] \nabla H/H \\
& + [l/h + F_M(d/h)] \nabla M_s/M_s - 2[l/h] \nabla \sigma_w/\sigma_w \},
\end{aligned} \quad (12)$$

where

$$F_h\left(\frac{d}{h}\right) = 6\left(\frac{h}{d}\right)I\left(\frac{d}{h}\right) - 3F\left(\frac{d}{h}\right) = 3J\left(\frac{d}{h}\right) \quad (13a)$$

$$\approx \frac{1}{\pi} \left\{ -\frac{9}{2} - \frac{3}{32} \left(\frac{h}{d}\right)^2 + \left[ 3 + \frac{9}{8} \left(\frac{h}{d}\right)^2 \right] \ln \left| \frac{4d}{h} \right| \right\}, \quad \frac{h}{d} \ll 1, \quad (13b)$$

$$\approx \frac{2}{\pi} \left(\frac{d}{h}\right)^2 - \frac{3}{8} \left(\frac{d}{h}\right)^3, \quad \frac{d}{h} \ll 1, \quad (13c)$$

$$F_H(d/h) = F(d/h), \quad (14)$$

and

$$F_M\left(\frac{d}{h}\right) = 4\left(\frac{h}{d}\right)I\left(\frac{d}{h}\right) - F\left(\frac{d}{h}\right), \quad (15a)$$

$$= \frac{1}{\pi} \left\{ -\frac{5}{2} + \frac{1}{32} \left(\frac{h}{d}\right)^2 + \left[ 3 + \frac{5}{8} \left(\frac{h}{d}\right)^2 \right] \ln \left| \frac{4d}{h} \right| \right\}, \quad \frac{h}{d} \ll 1, \quad (15b)$$

$$= \frac{d}{h} - \frac{2}{3\pi} \left(\frac{d}{h}\right)^2 + \frac{1}{64} \left(\frac{d}{h}\right)^5, \quad \frac{d}{h} \ll 1. \quad (15c)$$



Figure 4 shows plots of  $F_h$ ,  $F_M$  and  $F = F_H$  as functions of the normalized domain diameter. Numerical values of these functions are included in Table I. From the figure and the asymptotic forms of (7), (8), (13) and (14), it is seen that the functions are positive and that both  $F_h$  and  $F_H$  are greater than  $S_0(d/h)$ . From these properties and the stability requirement  $S_0(d/h) > l/h > S_2(d/h)$ , it is seen that for any stable domain the thickness gradient and magnetization gradient contributions to the force are in the direction of the gradient while the field gradient and wall energy gradient contributions to the force are in the direction opposite to the gradient.

The absolute value of each of the terms in equation (12) is small but measureable. If  $H_0$  and  $H_2$  are defined as the collapse and elliptical run-out fields respectively, then in the case of a gradient in the applied field where the stability limits are known roughly (see Ref. 5), the force produced on a domain for which  $d/h = 2$ ,  $h/l = 4$ ,  $\nabla H = (H_0 - H_2)/d$ ,  $d = 100$  microns and  $4\pi M_s = 100$  Gauss is approximately  $6 \times 10^{-3}$  dynes. While such absolute force measurements could possibly be carried out, a more relevant experiment for device applications is the balancing of field gradients against gradients in the other quantities. At the present time, no such measurements have been completed. However, the directions of the applied field gradient force, the wall energy gradient force, and the thickness gradient force have been verified. The sign of the  $H$  gradient force is verified in everyday device operation.

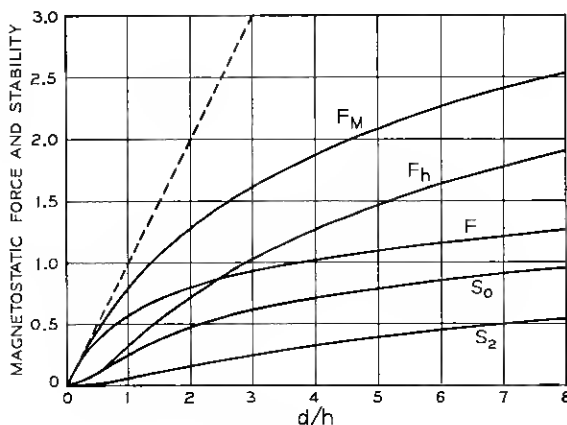


Fig. 4—The transverse magnetostatic force functions,  $F_M$ ,  $F_h$ , and  $F_H$  ( $F = F_H$ ) and the magnetostatic stability functions  $S_0$  and  $S_2$ , as functions of the diameter-to-thickness ratio.

The sign of  $\sigma_{10}$  gradient force was checked using a temperature gradient in a sample of  $\text{Sm}_{0.55}\text{Tb}_{0.45}\text{FeO}_3$ . According to the data of F. C. Rossol,<sup>7</sup> at room temperature the wall energy temperature coefficient is approximately  $+1.5\%/^\circ\text{C}$  and the magnetization is only a slightly decreasing function of temperature. The  $\sigma_{10}$  gradient force thus dominates in this material, and we observed that the domains move away from heated regions towards cooler regions as predicted. The sign of the  $M_s$  gradient force was verified using a temperature gradient in a sample of  $\text{Gd}_{2.3}\text{Tb}_{0.7}\text{Fe}_5\text{O}_{12}$  garnet. In this material  $M_s$  increases at  $3\%/^\circ\text{C}$  at room temperature while the wall energy is approximately constant. The  $M_s$  gradient force thus dominates, and we observed that the domains moved towards heated regions as predicted. The force direction measurements were completed in tapered platelets of orthoferrite in which we observed that the domains move towards the thick end of a platelet when restraints were removed.

It should be noted that in carrying out these experiments it is important to obtain low coercivity materials. This is especially true in measuring the thickness gradient force when  $\nabla h/h$  is small.

The drag force acting on a domain propagating with uniform velocity  $\mathbf{v}_d$  from equation 58 of Ref. 5 is given by

$$\mathbf{F}_d = -\frac{\pi}{2} d h M_s \left[ \frac{8}{\pi} H_c + \frac{2}{\mu_w} |\mathbf{v}_d| \right] \frac{\mathbf{v}_d}{|\mathbf{v}_d|}, \quad (16)$$

where  $H_c$  is the wall motion coercivity and  $\mu_w$  is the wall motion mobility. Equating to zero the sum of the gradient force (12) and the drag force (16) yields the velocity equation for an otherwise freely propagating domain. In order to avoid the vector sum in this equation, it is convenient to assume that all the gradients lie in the same direction and are positive. It is also convenient to assume that the gradients are uniform so that their magnitudes may be expressed in terms of the maximum parameter difference across the domain divided by the domain diameter,  $\nabla X = \Delta X/d$ . Under these assumptions the velocity equation is

$$\frac{8}{\pi} \frac{H_c}{4\pi M_s} + \frac{2 |\mathbf{v}_d|}{\mu_w 4\pi M_s} = C_h \frac{\Delta h}{h} - C_H \frac{\Delta H}{H} + C_M \frac{\Delta M_s}{M_s} - C_\sigma \frac{\Delta \sigma_w}{\sigma_w}, \quad (17a)$$

where

$$C_h = -\frac{h}{d} \left[ \frac{l}{h} - F_h \left( \frac{d}{h} \right) \right], \quad (17b)$$

$$C_H = -\frac{h}{d} \left[ \frac{l}{h} - F_H \left( \frac{d}{h} \right) \right], \quad (17c)$$

$$C_M = \frac{h}{d} \left[ \frac{l}{h} + F_M \left( \frac{d}{h} \right) \right], \quad (17d)$$

and

$$C_\sigma = 2 \frac{h}{d} \frac{l}{h} = \frac{l}{r_0} \quad (17e)$$

are called transverse force coefficients and are all positive.

For a domain having the diameter  $d = 8l$  in a plate of thickness  $4l$ , the velocity equation becomes

$$\begin{aligned} \frac{8}{\pi} \frac{H_c}{4\pi M_s} + \frac{2 |\mathbf{v}_d|}{\mu_w 4\pi M_s} \\ = 0.238 \frac{\Delta h}{h} - 0.279 \frac{\Delta H}{H} + 0.772 \frac{\Delta M_s}{M_s} - 0.250 \frac{\Delta \sigma_w}{\sigma_w}. \end{aligned} \quad (18)$$

If the magnitude of the sum of the gradients is not sufficiently large, no motion takes place. For example, when a domain having dimensions such that equation (18) applies is subjected to a field gradient, the magnitude of the field difference across the domain must satisfy the condition  $\Delta H/H > 9.1 \times H_c/4\pi M_s$  before any motion can take place.

The transverse force coefficients are plotted as functions of the normalized thickness  $h/l$  in Fig. 5 for the bias condition  $d = (d_0 d_2)^{1/2}$  where  $d_0$  and  $d_2$  are the collapse and elliptical runout diameters respectively. For small thicknesses the asymptotic forms of  $C_h$ ,  $C_M$ , and  $C_\sigma$  are proportional to  $(l/h) \exp(-\pi l/h)$  and the asymptote of  $C_H$  is proportional to  $\exp(-\pi l/h)$ . For large thicknesses  $C_H$  and  $C_M$  approach unity, and  $C_\sigma$  and  $C_h$  approach the asymptote  $(8/3\pi)^{1/2} (l/h)^{1/2}$ .

Some caution must be exercised in interpreting equation (17) and Fig. 5. First, the stability of moving domains has only been investigated for the case of gradients in the applied field and then only incompletely (see Ref. 5). Another problem is that drive gradients which are applied from the surface and which must obey Laplace's equation, such as field gradients and temperature gradients, decrease exponentially into the platelet. (This does not apply to volume heating such as laser heating.) For any given value of these gradients at the surface the maximum  $z$  averaged value of these gradients which may be applied thus decreases according to the inverse first power of the plate thickness in thick plates. This consideration shows that the use of platelets having a thickness no greater than the preferred thickness of  $4l$  is thus more strongly preferred for achieving a high domain velocity than is indicated by inspection of Fig. 5 alone.

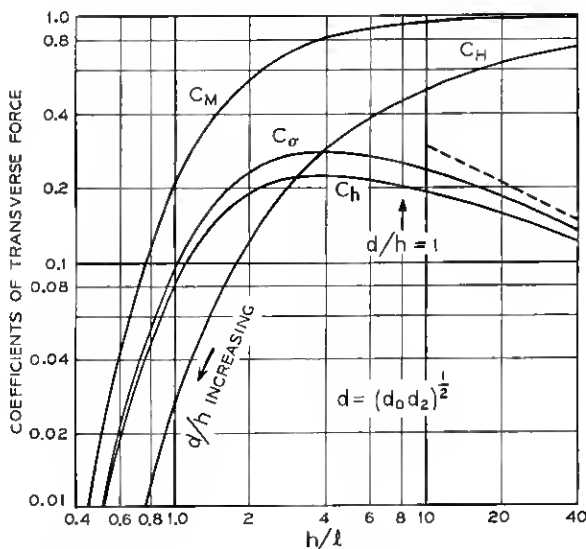


Fig. 5—The transverse force coefficients  $C_h$ ,  $C_H$ ,  $C_M$ , and  $C_\sigma$  for the bias condition  $d = (d_0 d_2)^{1/2}$ , as functions of the normalized thickness,  $h/l$ .

#### IV. SIGNIFICANCE FOR DEVICE APPLICATIONS

Equation (17) and Fig. 5, when properly interpreted, show again that there is a preferred plate thickness for achieving high bit rates in devices and that this thickness is again  $4l$ . Equation (18) shows that, for plates of this thickness, wall energy, magnetization and applied field gradients produce transverse forces of similar magnitude. Figure 5 shows that this is also true for plates having a thickness in the neighborhood of  $4l$ . There is therefore no preferred thickness with respect to favoring applied field gradients over temperature or composition gradients.

In temperature dependent materials in which the domain tends to move towards the high temperature direction the domain will tend to follow a laser beam initially placed at its center. In materials having the opposite temperature characteristic, the domains may be pushed by a laser beam. Gradients in thickness or composition may be used to define domain tracks in order to increase margins with respect to spurious field or temperature gradients. An immediately useful application of equation (18) is in the calculation of the effect on device margins of the heat produced by domain generators and detectors.

## APPENDIX

*The Internal Magnetostatic Energy Function*

Various representations of the internal magnetostatic energy function,  $I(d/h)$ , are given in this appendix. Since  $F(d/h)$  is non-negative (Ref. 3, Fig. 3 and equation 138), the integral definition of  $I(d/h)$  (2) implies that  $I(d/h)$  is positive and monotonic increasing as can be seen in Fig. 1. (Neither function is defined in the present case for negative values of the argument.) The definition of  $I(d/h)$  also implies the differential equation,  $dI(x)/dx = F(x)$ , with the boundary condition  $I(0) = 0$ . The internal magnetostatic function may be written as

$$I\left(\frac{d}{h}\right) = -\frac{1}{3\pi} \frac{d}{h} \left[ 2 \frac{d^2}{h^2} + \left(1 - \frac{d^2}{h^2}\right) U\left(\frac{h^2}{d^2}\right) - \left(1 + \frac{h^2}{d^2}\right) V\left(\frac{h^2}{d^2}\right) \right], \quad (19)$$

where as in equations (84) and (85) of Ref. 3

$$U(x) \equiv 2(x+1)^{\frac{1}{2}} E\left(\frac{1}{1+x}\right), \quad (20a)$$

and

$$V(x) \equiv 2(x+1)^{-\frac{1}{2}} K\left(\frac{1}{1+x}\right), \quad (20b)$$

where  $K(m)$  and  $E(m)$  are the complete elliptic integrals of the first and second kind respectively and the argument is in the  $m$  of Ref. 8. Differentiation of equation (19) with respect to  $d/h$  and combining terms using equations (86) and (87a) of Ref. 3 verifies that the derivative of  $I(d/h)$  is indeed  $F(d/h)$  (equation 138 of Ref. 3). Substitution of the series expansions of  $U$  and  $V$  (equations 96 and 97 of Ref. 3) verifies that  $I(0) = 0$ .

Writing  $I(d/h)$  in terms of the  $L_1$  function (Ref. 3 Sec. A.4) eliminates the negative power of  $d/h$ ,

$$I\left(\frac{d}{h}\right) = \frac{1}{3\pi} \frac{d}{h} \left\{ \left(\frac{d}{h}\right)^2 \left[ U\left(\frac{h^2}{d^2}\right) - 2 \right] - \frac{1}{2} L_1\left(\frac{h^2}{d^2}\right) + V\left(\frac{h^2}{d^2}\right) \right\}, \quad (21)$$

and the expression in terms of  $F(d/h)$  and  $S_0(d/h)$  (equations 138 and 139 of Ref. 3) is also sometimes useful,

$$I\left(\frac{d}{h}\right) = \frac{1}{3} \frac{d}{h} \left\{ 2F\left(\frac{d}{h}\right) + S_0\left(\frac{d}{h}\right) \left[ 1 + \frac{h^2}{d^2} \right] - \frac{2}{\pi} \right\}. \quad (22)$$

The power series expansions of  $I(d/h)$  may be determined either by substituting the power series expansions for  $U$ ,  $V$  and  $L_1$  (Ref. 3, Sections A.3 and A.4) into equation (21) or by term-by-term integration of  $F(d/h)$  with the integration constants being determined from the lowest order terms of the power series expansions of  $U$  and  $V$ . The result is

$$I\left(\frac{d}{h}\right) = \frac{1}{\pi} \left\{ \left[ -\frac{1}{2} \left(\frac{d}{h}\right) + \frac{1}{32} \left(\frac{h}{d}\right) + \frac{1}{96} \left(\frac{h}{d}\right)^3 - \frac{109}{24576} \left(\frac{h}{d}\right)^5 + \dots \right] \right. \\ \left. + \left[ \left(\frac{d}{h}\right) + \frac{1}{8} \left(\frac{h}{d}\right) - \frac{1}{64} \left(\frac{h}{d}\right)^3 + \frac{5}{1024} \left(\frac{h}{d}\right)^5 + \dots \right] \ln \left| \frac{4d}{h} \right| \right\} \quad (23a)$$

$$= \frac{1}{2} \left(\frac{d}{h}\right)^2 - \frac{2}{3\pi} \left(\frac{d}{h}\right)^3 + \frac{1}{16} \left(\frac{d}{h}\right)^4 - \frac{1}{128} \left(\frac{d}{h}\right)^6 + \frac{5}{2048} \left(\frac{d}{h}\right)^8 + \dots \quad (23b)$$

#### REFERENCES

1. Bobeck, A. H., Fischer, R. F., Perneski, A. J., Remeika, J. P., and Van Uitert, L. G., "Application of Orthoferrites to Domain-Wall Devices," *IEEE Trans. Magnetics*, **5**, No. 3 (September 1969), pp. 544-553.
2. Perneski, A. J., "Propagation of Cylindrical Magnetic Domains in Orthoferrites," *IEEE Trans. Magnetics*, **5**, No. 3 (September 1969), pp. 554-557.
3. Thiele, A. A., "The Theory of Cylindrical Magnetic Domains," *B.S.T.J.*, **48**, No. 10 (December 1969), pp. 3287-3335.
4. Thiele, A. A., "Theory of the Static Stability of Cylindrical Domains in Uniaxial Platelets," *J. Appl. Phys.*, **41**, No. 3 (March 1970), pp. 1139-1145.
5. Thiele, A. A., "Device Implications of the Theory of Cylindrical Magnetic Domains," *B.S.T.J.*, this issue, pp. 725-773.
6. Cape, J. A., and Lehman, G. W., "Magnetic Bubble Domain Interactions," *Solid State Commun.*, **8**, No. 16 (August 1970), pp. 1303-1306.
7. Rossol, F. C., "Temperature Dependence of Rare-Earth Orthoferrite Properties Relevant to Propagating Domain Device Applications," *IEEE Trans. Magnetics*, **5**, No. 3 (September 1969), pp. 562-565.
8. *Handbook of Mathematical Functions*, Abramowitz, M., and Stegun, J. A., editors, Nat. Bureau of Standards Appl. Math. Series 55, Washington, D. C., 1966, pp. 589-626.